16

FERMILAB

JAN 18 2001

LIBRARY

GANIL

GANIL-P-00-45

Isospin dependence of the microscopic JLM model

A. Pakou[a,c,1], N. Alamanos[b], P. Roussel-Chomaz[c], F. Auger[b], D. Rosengrant[b,2] and A. de Vismes[c]

[a] *Department of Physics, The University of Ioannina, 45110 Ioannina, Greece*
[b] *CEA/DSM/DAPNIA/SPhN, Saclay, 91191 Gif-sur-Yvette Cedex, France*
[c] *GANIL (DSM/CEA, IN2P3/CNRS), BP 5027 Caen Cedex, France*

Fermilab Library
0 1160 0089368 9

Submitted to Physics Letters

GANIL P 00 45

Isospin dependence of the microscopic JLM model

A. Pakou[a,c,1], N. Alamanos[b], P. Roussel-Chomaz[c], F. Auger[b], D. Rosengrant[b,2] and A. de Vismes[c]

[a] *Department of Physics, The University of Ioannina, 45110 Ioannina, Greece*

[b] *CEA/DSM/DAPNIA/SPhN, Saclay, 91191 Gif-sur-Yvette Cedex, France*

[c] *GANIL (DSM/CEA, IN2P3/CNRS), BP 5027 Caen Cedex, France*

[1] corresponding author, apakou@cc.uoi.gr

[2] On leave, University of Pittsburgh, Pittsburgh PA 15260 USA

Abstract

A systematic study of elastic proton and neutron scattering as well as (p,n) charge exchange reactions was undertaken in the context of the JLM microscopic framework in order to test the isovector part of the potential. The study included the stable nuclei ^{48}Ca, ^{90}Zr, ^{120}Sn and ^{208}Pb in the energy range of ~25-45 MeV and the halo nucleus ^{6}He at ~40 MeV. It was found that the stable nuclei data can be reproduced, by an adjustment of the isovector part through a renormalization factor, $\lambda_{isov} \sim$ 2-2.5. The required isovector adjustment for the halo nucleus data will be discussed.

PAC Numbers: 25.40.Cm,25.40.Dn,25.40.Kv,21.30.Fe

KEYWORDS: microscopic potential, isovector potential, (p,n) angular distributions, (p,p) angular distributions, (n,n) angular distributions, halo nuclei.

It is well known that in the context of the Lane model [1] a consistent description of proton elastic scattering and charge exchange reactions can provide information on the isoscalar and isovector part of the nucleon-nucleon interaction and can also, to some extent, probe differences between the proton and neutron density distributions [2]. With the advent of radioactive beam facilities, a good knowledge of the isoscalar and isovector part of the potential is necessary in order to probe properties of nuclei near the drip line.

However, while nucleon scattering is adequately described by several theories, the interpretation of (p,n) charge exchange reactions into a phenomenological or microscopic framework have met with limited success [3, 4, 5, 6, 7].

The microscopic JLM approach, which was derived by Jeukenne, Lejeune and Mahaux [8, 9], has been extensively studied by Hansen et al. [10] and Petler et al. [11]. It has been particularly successful in describing elastic proton and neutron scattering for stable nuclei with slight adjustments, mainly on the imaginary part of the central potential and with no adjustment on the strength of the isovector term [12]. Moreover, it was established previously by Alamanos et al. [13] the adequacy of JLM to describe elastic and also inelastic proton scattering, by using measured transition density distributions. On the other hand, no systematic study exists for (p,n) charge exchange reactions, in the framework of the JLM model. Calculations performed in the past for ^{208}Pb [14], seem to reproduce the angular distribution structure of the (p,n) reaction but fail to reproduce the absolute magnitude of the cross section by a factor of 4 to 6 [14]. The origin of this discrepancy was attributed by the authors to the very weak ratio of the real isovector to isoscalar term of the JLM approach, which was significantly smaller than that found in phenomenological potentials [15, 16, 17, 18] and the M3Y interaction [19], by a factor of ~2.

Thus, to clarify the situation we report in this letter a systematic study of (p,p) and (n,n) elastic scattering as well as (p,n) charge exchange reactions

in a wide mass range of stable systems (A=48-208) and attempt to apply our findings to the halo nucleus ^{6}He.

JLM microscopic calculations were performed in a microscopic DWBA approach, in which entrance- and exit- channel optical potentials are calculated consistently using an energy and density dependent interaction. This interaction was derived from the nuclear matter calculation of Jeukenne, Lejeune and Mahaux [8, 9]. The starting point for computing the JLM potentials, is the Brueckner-Hartree-Fock approximation and the Reid hard core nucleon-nucleon interaction which provides, for energies up to 160 MeV, the energy and density dependence of the isoscalar, isovector and Coulomb components of the complex optical potential in infinite matter. The optical potential of a finite nucleus is obtained by making the local density approximation (LDA), that is substituting the nuclear matter density with the density distribution of the nucleus and including the effect of the range of the effective interaction in a phenomenological way [9].

Our present calculations span a broad mass range, including the nuclei ^{48}Ca, ^{90}Zr, ^{120}Sn and ^{208}Pb at various proton energies. It would have been desirable to extend our study to lighter systems, but this was not possible due to lack of (p,n) data on isobaric analog states. Density distributions were constructed by adopting typical Fermi type distributions and making use of electron scattering results [20, 21]. For ^{208}Pb the proton density was derived from Frois et al. [22] and the neutron density from Hoffmann et al. [23] according to the suggestion of ref. [24]. The (p,p) elastic scattering calculations are displayed in Fig. 1, the (n,n) ones in Fig. 2 and the (p,n) results in Fig. 3 and 4, and are compared with experimental values determined previously [25, 26, 27, 28, 29, 30, 31]. The calculations were done by adopting real and imaginary normalization factors equal to λ_v=1.0, λ_w=0.8 for the lighter isotopes and λ_v=λ_w=1.0 for the heavier ones. Initially no adjustment was applied to the isovector part (dashed lines). As it can be seen from all figures and in agreement with previous results for (p,p) and (n,n) elastic scattering [10, 11, 12], the calculations describe adequately well the (p,p) angular distribution results and present also a fair compatibility with the (n,n) ones. As for the (p,n) charge exchange reaction data, although they describe the shape of the angular distribution well, they underestimated the cross sections by approximately an order of magnitude. Thus the calculations were repeated with an isovector adjustment for both the real and imaginary part, $\lambda_{isov} \sim$ 2-2.5. In this way the increase obtained for the (p,n) cross section strength made the calculations compatible with the experimental values, while no apparent change occurred for the (p,p) elastic scattering and small improvements were observed for the (n,n) one. Our result, for the requested increase of the isovector strength, confirms previous findings reported by F.S Dietrich et al. [14] for the ^{208}Pb(p,n)^{208}Bi reaction, and brings this strength closer to phenomenological descriptions [15, 16, 17] and the M3Y interaction. The obtained potentials are summarized in Table 1. It must be pointed out here that a systematic weak energy dependence is seen on the isovector adjustment, since

for the 25 MeV (p,n) data the isovector normalization factor was 2, while for the 35 and 45 MeV data the requested renormalization was 2.5.

To further extend our study, reaction cross section calculations were also undertaken adopting the potentials of Table 1 and are shown in Table 2. For reasons of completeness the calculations were repeated for λ_{isov}=1.0 and are also shown in the same table, where they are compared with previously measured values [32]. The overall agreement is adequately good for the higher energies and fairly good for the lower ones. The general trend confirms the adjustment of the isoscalar part made in the (p,n) data, although the differences between values determined with λ_{isov}=2.5 and λ_{isov}=1.0 are of the same order of magnitude with the errors assigned to the measured values .

Subsequently, we focused our attention on the halo nucleus ^{6}He. A systematic study of the JLM optical potential of this nucleus will be published elsewhere [33], by combining data obtained by different reaction techniques as proton elastic scattering and (p,n) distributions as well as a new reaction cross section measurement (σ_R=409±22mb). The (p,n) and reaction cross section data were well reproduced by an isovector adjustment equal to λ_{isov}=1.4 for three different halo densities, namely a shell model one [34] and two cluster model densities [35, 36]. The adjustment was applied both for the real and imaginary part.

An explanation for the reduction of the isovector adjustment from the value obtained for the stable isotopes, could possibly be attributed on the large spatial extension of the neutron distribution, which characterizes ^{6}He. This is quite plausible, because as it has been reported elsewhere [14], the isovector normalization adjustment is density dependent and increases with decreasing density. To test this hypothesis we have attempted to construct gaussian density distributions assuming a) equal r.m.s matter and neutron radii to the proton radius, r.m.s=1.9 fm, that is treating the ^{6}He nucleus as a standard stable nucleus b) equal r.m.s proton and neutron radii to the matter radius, r.m.s=2.52 fm, that is treating the ^{6}He nucleus as a standard stable nucleus but with more extended spatial distributions and c) different proton and neutron radii, r.m.s$_p$=1.9 fm and r.m.s$_n$=2.8 fm, adopting a structure more adequate for this abnormal neutron excess nucleus with radii similar to those predicted in theory [34, 35, 36] and close to experimental values [37, 38]. With these three distributions we repeated the calculations for the proton elastic scattering data, the reaction cross section measurement and the (p,n) angular distribution. In order to reproduce all the data it was found necessary to increase the isovector normalization factor in case a) by 40 % to the value of λ_{isov}=2 compatible with the stable nuclei results, in case b) by 18% to the value λ_{isov}=1.65 while in case c) no increase was found necessary and the results were described as for the halo shell model and cluster density distributions with λ_{isov}=1.4. It has to be pointed out here that the isovector adjustment is independent of the adopted real and imaginary normalization factors of the isoscalar potential, into a maximum uncertainty of 7%. The previous and present (p,n) calculations appear in Fig. 5. The errors

assigned to the (p,n) data at backward angles ($\theta_{cm} \geq 15^0$) were increased from our previous publication [39] due to difficulties in estimating the efficiency. However the data at small angles are well determined and they are reproduced with both halo and the non halo densities of case a) and b) with smaller and larger spatial distributions, as long as the isovector adjustment is 1.4 , 2.0 and 1.65 respectively. This set of values (2.0, 1.65, 1.4) clearly indicates the sensitivity of the isovector adjustment on the spatial extension of the distribution and raises the question as to weather the nuclear-matter approach (LDA approximation) can yield accurate predictions of the isovector interaction. An interesting point however has to be noticed here concerning the potential of such calculations. Since the shape of the angular distribution is preserved, as has been demonstrated previously for the angular distributions of stable nuclei, irrespectively of the isovector adjustment, the isovector renormalization can be fixed through fits to the forward angular distribution data. Subsequently the data at larger angles can be used in principle to probe differences between various types of densities. This after all is the bottom line of such type of calculations [2], concerning especially halo nuclei. However in the present case of ^{6}He due to the large errors assigned to the data beyond 15^0, no conclusions can be drawn for the adequacy of specific densities.

It has been shown that in the JLM theoretical framework, a consistent description of (p,p), (n,n), (p,n) and reaction cross section data of stable nuclei spanning a broad mass range (A=48-208) can be obtained by adopting an isovector renormalization factor of the order $\lambda_{isov} \sim$ 2-2.5, depending on the energy. This adjustment brings the isovector over the isoscalar strength of the interaction closer to both phenomenological potentials and the M3Y interaction. The situation appears more complicated for the halo nuclei, pointing out the limitations of the nuclear-matter approach adopted in the JLM theory. Due to the abnormal neutron excess of ^{6}He and to the sensitivity of the isovector part on the density, a reduced normalization factor equal to λ_{isov}=1.4 was obtained. This normalization factor can not be used a priori for other halo nuclei. However, despite these shortcomings of the interaction, (p,n) charge exchange reaction data can be used safely to probe density differences. This can be achieved by fixing the isovector potential at small scattering angles of the (p,n) angular distribution and then observing the density differences at larger angles. Obviously new (p,n) data at larger angles and of better statistics are necessary to test the difference between neutron and proton density distribution for the halo nucleus ^{6}He.

Acknowledgement

One of us (A. Pakou) would like to acknowledge Prof. P. Assimakopoulos for reading carefully this manuscript

References

[1] A. M. Lane, Nucl. Phys. **35**, 676 (1962).

[2] C. J. Batty *et al.*, Advances in Nuclear Physics **19**, 1 (1989).

[3] G. W. Hoffmann and W. R. Coker, Z. Phys. **269**, 307 (1974).

[4] G. W. Hoffmann and W. R. Coker, Phys. Rev. Lett. **29**, 227 (1972).

[5] C. Wong, S. M. Grimes, R.W. Finley, Phys. Rev. C **29**, 1710 (1984).

[6] D. Carlson, C.D. Zafiratos, Nucl. Phys. **A249**, 29 (1975).

[7] D. Schery *et al.*, Nucl. Phys. **A234**, 109 (1974).

[8] J. P. Jeukeune, A. Lejeune and C. Mahaux, Phys. Rev C **16**, 80 (1977).

[9] N. Alamanos and P. Roussel-Chomaz, Ann. Phys. Fr. **21**, 601 (1996).

[10] L.F. Hansen *et al.*, Phys. Rev C **31**, 111 (1985).

[11] J.S. Petler *et al.*, Phys. Rev C **32**, 673 (1985).

[12] S. Mellema *et al.*, Phys. Rev C **28**, 2267 (1983).

[13] N. Alamanos *et al.*, Nucl. Phys. **A660**, 406 (1999).

[14] F. S. Dietrich and F. Petrovich, in proceedings of Neutron-Nucleus Collisions -a probe of nuclear structure, eds J. Rapaport et al., AIP Conference Proceedings, **124** 90 (AIP, New York, 1985).

[15] F. D. Becchetti and G. W. Greenlees, Phys. Rev **182**, 1190 (1969).

[16] J. Rapaport *et al.*, Nucl. Phys. **A330**, 15 (1979).

[17] S. Austin, An Empirical Effective interaction in Proceedings "The (p,n) Reaction and the Nucleon-Nucleon force" eds C. D. Goodman *et al.*, Plenum Press , 203 1980).

[18] R. L. Varner *et al.*,Phys. Rep. **201**, 57 (1991).

[19] G. R. Satchler and W. G. Love, Phys. Rep. **55** (1979) 183.

[20] H. De Vries et al., Atomic and Nuclear Data Tables **36**, 495 (1987).

[21] C. W. de Jager *et al.*, Atomic and Nuclear Data Tables **14**, 479 (1974).

[22] B. Frois *et al.*, Phys. Rev. Lett. **38**, 152 (1977).

[23] G. W. Hoffmann *et al.*, Phys. Rev. C **21**, 1488 (1980).

[24] F. S. Dietrich *et al.*, Phys. Rev. Lett. **51**, 1629 (1983).

[25] C. R. Gruhn *et al.*, Phys. Rev. C **6**, 944 (1972).

[26] M.P. Fricke *et al.*, Phys. Rev. **156**, 1207 (1967).

[27] L.N. Blumberg *et al.*, Phys. Rev. **147**, 812 (1966).

[28] R.R. Doering *et al.*,Phys. Rev. C **12**, 378 (1975).

[29] D.E. Bainum *et al.*, Phys. Rev. C **16**, 1377 (1977).

[30] P.P. Guss *et al.*, Phys. Rev. C **39**, 405 (1989).

[31] S.F. Hicks *et al.*, Phys. Rev. C **41**, 2560 (1990).

[32] R. F. Carlson, Atomic Data and Nuclear Data Tables **63**, 94 (1996).

[33] Anne des Vismes *et al.*, to be published

[34] S. Karataglidis *et al.*,Phys. Rev. C **61**, 024319 (2000) .

[35] J. S. Khalili and J. A. Tostevin Phys. Rev. C **57**, 1846 (1998).

[36] K. Arai *et al.*, Phys. Rev. C **59**, 1432 (1999).

[37] I. Tanihata *et al.*, Phys. Lett. B **206**, 592 (1988).

[38] I. Tanihata *et al.*, Phys. Lett. B **289**, 261 (1992).

[39] M.D. Cortina-Gil *et al.*, Nucl. Phys. **A641**, 263 (1998).

1 FIGURE CAPTIONS

Fig. 1 JLM calculations for proton elastic scattering at different energies and for various nuclei. Dashed lines correspond to λ_{isov}=1.0, solid lines to λ_{isov}=2.5. The similarity of the calculations shows that they are not sensitive on the isovector term. Calculations were done for the lighter isotopes with λ_v=1.0 and λ_w=0.8 and for the heavier ones with λ_v=λ_w=1.0 (see Table I). The data are from ref. [25, 26, 27].

Fig. 2 JLM calculations for neutron elastic scattering for various nuclei. Dashed lines correspond to λ_{isov}=1.0, solid lines to λ_{isov}=2.5 for ^{48}Ca, ^{208}Pb and to λ_{isov}=2.0 for ^{90}Zr, ^{120}Sn. Calculations were done for the lighter isotopes with λ_v=1.0 and λ_w=0.8 and for the heavier ones with λ_v=λ_w=1.0 (see Table 1). The data are from ref. [29, 30, 31].

Fig. 3 JLM calculations for (p,n) charge exchange reactions for ^{48}Ca and ^{90}Zr at 25, 35 and 45 MeV. Dashed lines correspond to λ_{isov}=1.0, solid lines to λ_{isov}=2.0 for the 25 MeV data and λ_{isov}=2.5 for the 35 and 45 MeV ones. Calculations were done with λ_v=1.0 and λ_w=0.8 (see Table 1). The data are from ref. [28].

Fig. 4 JLM calculations for (p,n) charge exchange reactions for ^{120}Sn and ^{208}Pb at 25, 35 and 45MeV. Dashed lines correspond to λ_{isov}=1.0, solid lines to λ_{isov}=2.0 for the 25 MeV data and λ_{isov}=2.5 for the 35 and 45 MeV ones. Calculations were done with λ_v=λ_w=1.0 (see Table 1). The data are from ref. [28].

Fig. 5 JLM calculations for the ^{6}He(p,n)^{6}Li charge exchange reaction. The solid line corresponds to a shell model halo density distribution [34] with λ_{isov}=1.4. The lines for the two other halo densities [35, 36] were inseparable at low momentum transfer and they are not shown in this figure. The other three lines the dashed, dotted and dotted-dashed correspond to the gaussian distributions of case a), b) and c) (see text) and was done for λ_{isov}=2.0, 1.65 and 1.4 respectively. The data are from ref. [39].

nucleus	λ_v	λ_W	E_p(MeV)	λ_{isov}
^{48}Ca	1.0	0.8	25.0	2.0
^{48}Ca	1.0	0.8	35.0	2.5
^{48}Ca	1.0	0.8	45.0	2.5
^{90}Zr	1.0	0.8	25.0	2.0
^{90}Zr	1.0	0.8	35.0	2.5
^{90}Zr	1.0	0.8	45.0	2.5
^{120}Sn	1.0	1.0	25.0	2.0
^{120}Sn	1.0	1.0	35.0	2.5
^{120}Sn	1.0	1.0	45.0	2.5
^{208}Pb	1.0	1.0	25.0	2.0
^{208}Pb	1.0	1.0	35.0	2.5
^{208}Pb	1.0	1.0	45.0	2.5

TABLE 1. JLM potentials, adopted through the proton, neutron elastic scattering and the (p,n) charge exchange reaction study.

nucleus	E_p(MeV)	$\sigma_{calculated}$(mb) λ_{isov}=2.5	λ_{isov}=1.0	$\sigma_{measured}$(mb)
^{48}Ca	30.3	1011	953	999±55
	45.3	894	835	908±34
^{90}Zr	30.0	1331	1294	1249±45
	40.0	1307	1262	1316±65
^{120}Sn	30.0	1557	1517	1589±50
	40.0	1593	1543	1618±73
^{208}Pb	30.0	1858	1785	2117±90
	40.0	2043	1961	2023±100

TABLE 2. Calculated reaction cross sections into the JLM framework, adopting the potentials of Table 1, are compared with measured values [32].

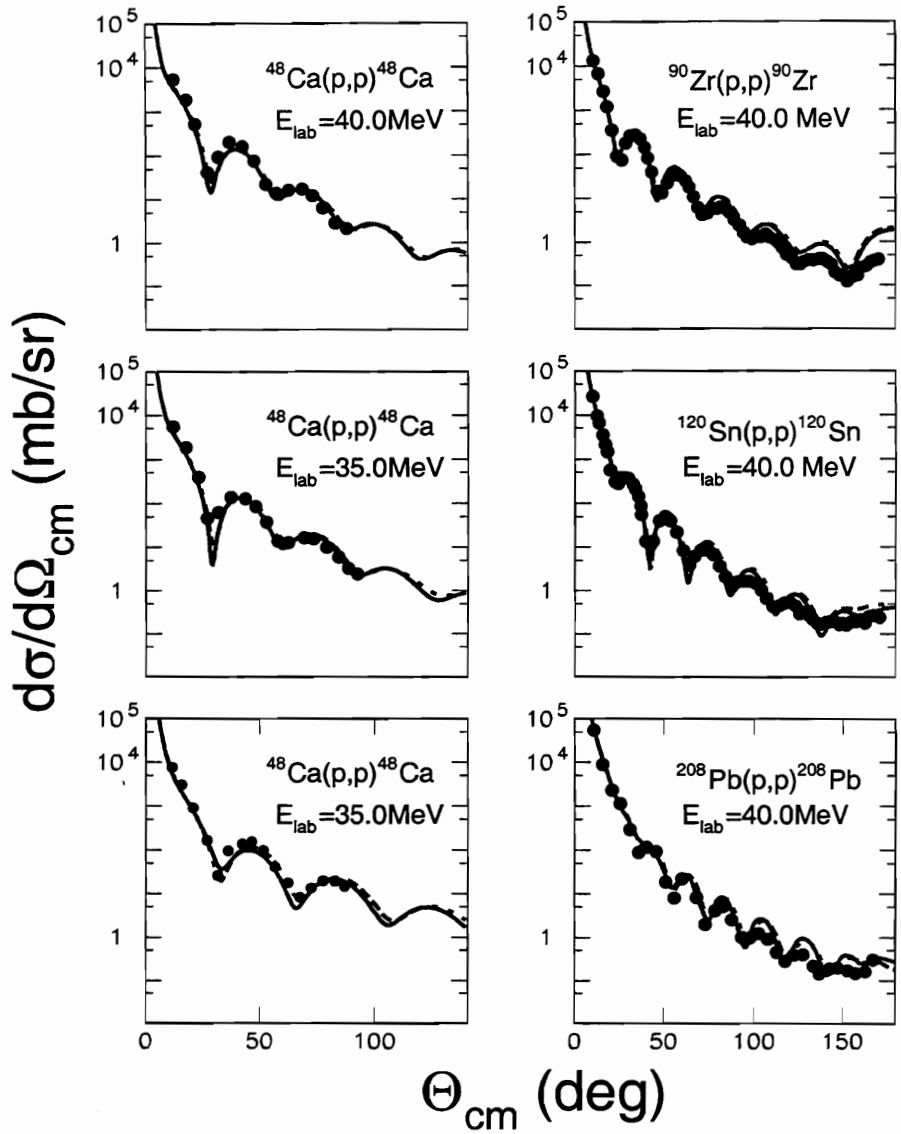
^{48}Ca(p,p)^{48}Ca
E_{lab}=40.0MeV
^{90}Zr(p,p)^{90}Zr
E_{lab}=40.0 MeV
^{48}Ca(p,p)^{48}Ca
E_{lab}=35.0MeV
^{120}Sn(p,p)^{120}Sn
E_{lab}=40.0 MeV
^{48}Ca(p,p)^{48}Ca
E_{lab}=35.0MeV
^{208}Pb(p,p)^{208}Pb
E_{lab}=40.0MeV
$d\sigma/d\Omega_{cm}$ (mb/sr)
Θ_{cm} (deg)

Fig. 1

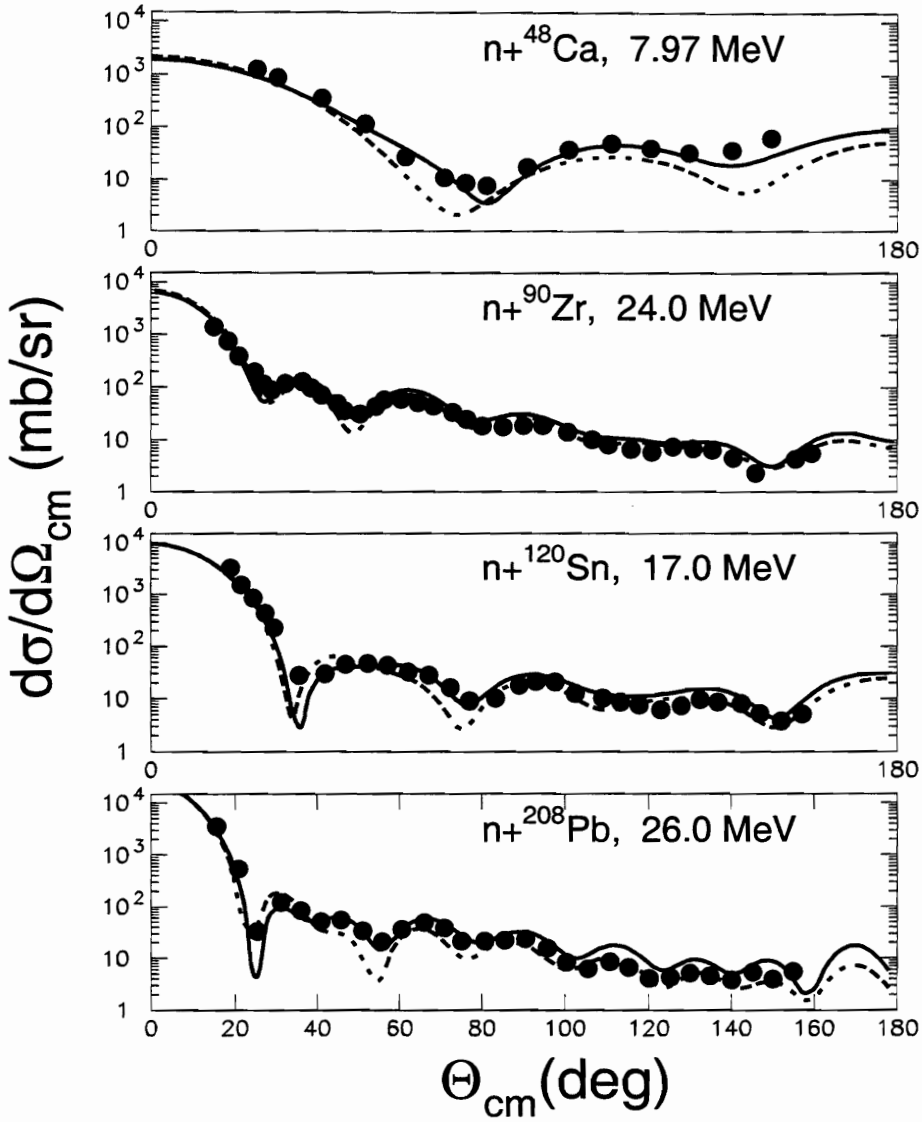
n+48Ca, 7.97 MeV
n+90Zr, 24.0 MeV
n+120Sn, 17.0 MeV
n+208Pb, 26.0 MeV
dσ/dΩcm (mb/sr)
Θcm(deg)

Fig. 2

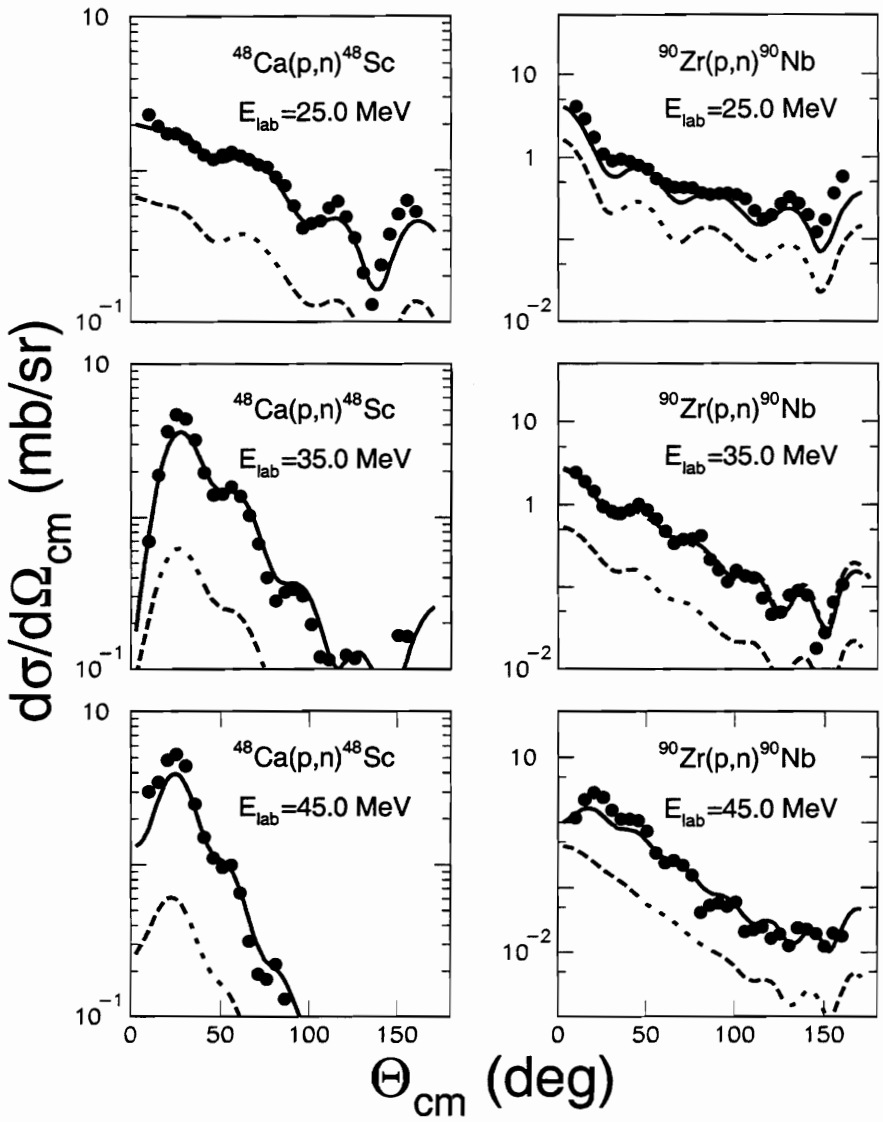
^{48}Ca(p,n)^{48}Sc
E_{lab}=25.0 MeV
^{90}Zr(p,n)^{90}Nb
E_{lab}=25.0 MeV
^{48}Ca(p,n)^{48}Sc
E_{lab}=35.0 MeV
^{90}Zr(p,n)^{90}Nb
E_{lab}=35.0 MeV
^{48}Ca(p,n)^{48}Sc
E_{lab}=45.0 MeV
^{90}Zr(p,n)^{90}Nb
E_{lab}=45.0 MeV
$d\sigma/d\Omega_{cm}$ (mb/sr)
Θ_{cm} (deg)
10
1
10^{-1}
10^{-2}
0
50
100
150

Fig. 3

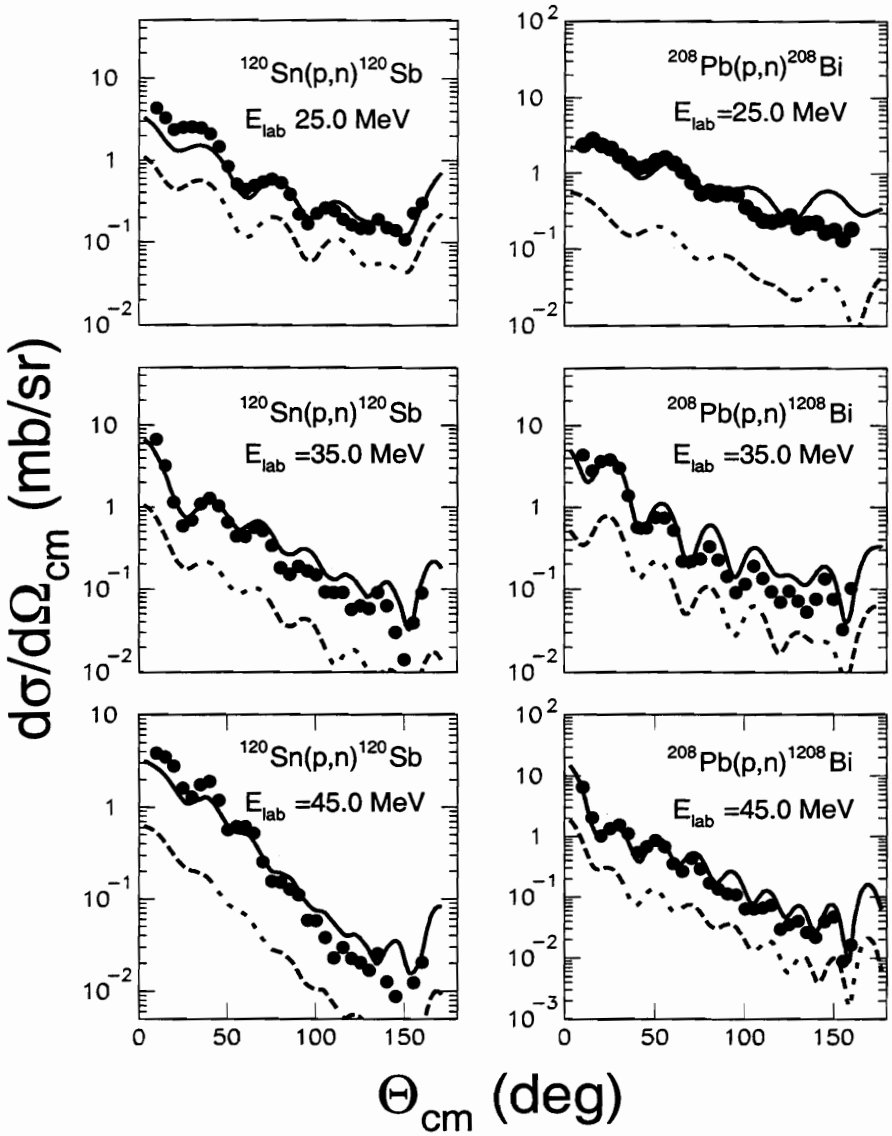
^{120}Sn(p,n)^{120}Sb
E_{lab} 25.0 MeV
^{208}Pb(p,n)^{208}Bi
E_{lab}=25.0 MeV
^{120}Sn(p,n)^{120}Sb
E_{lab} =35.0 MeV
^{208}Pb(p,n)^{1208}Bi
E_{lab} =35.0 MeV
^{120}Sn(p,n)^{120}Sb
E_{lab} =45.0 MeV
^{208}Pb(p,n)^{1208}Bi
E_{lab} =45.0 MeV
$d\sigma/d\Omega_{cm}$ (mb/sr)
Θ_{cm} (deg)

Fig. 4

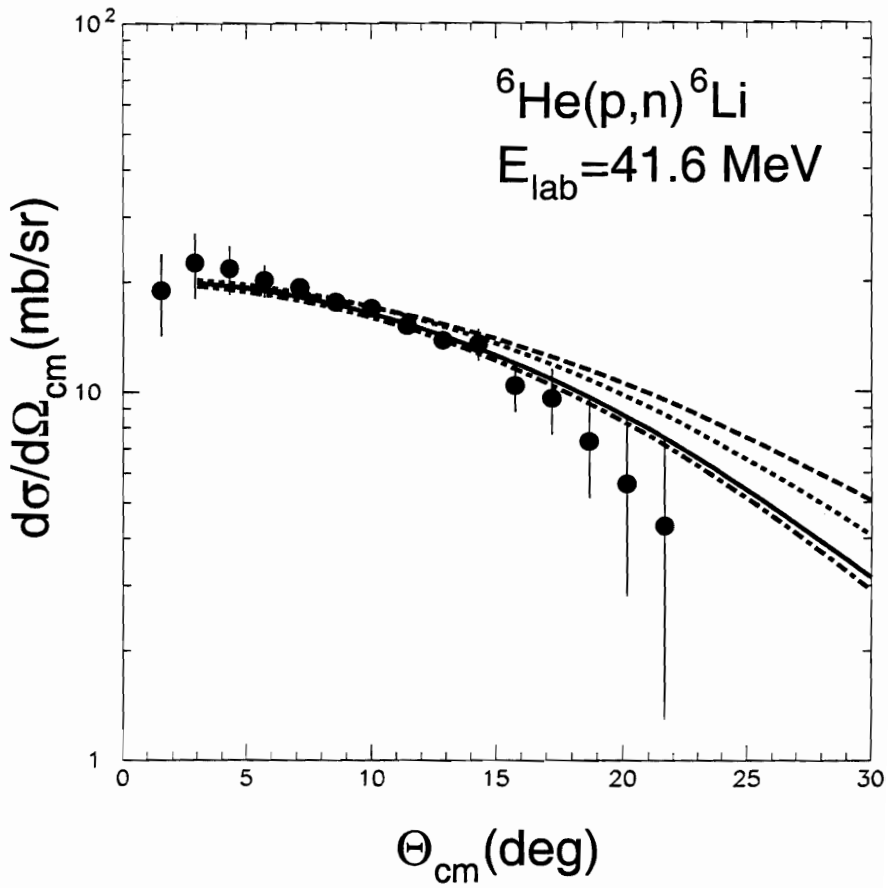
^{6}He(p,n)^{6}Li
E_{lab}=41.6 MeV
$d\sigma/d\Omega_{cm}$(mb/sr)
Θ_{cm}(deg)
10^2
10
1
0
5
10
15
20
25
30

Fig. 4